

REPORT DOCUMENTATION PAGE					Form Approved OMB No. 0704-0188	
<p>The public reporting burden for this collection of information is estimated to average 1 hour per response, including the time for reviewing instructions, searching existing data sources, gathering and maintaining the data needed, and completing and reviewing the collection of information. Send comments regarding this burden estimate or any other aspect of this collection of information, including suggestions for reducing the burden, to Department of Defense, Washington Headquarters Services, Directorate for Information Operations and Reports (0704-0188), 1215 Jefferson Davis Highway, Suite 1204, Arlington, VA 22202-4302. Respondents should be aware that notwithstanding any other provision of law, no person shall be subject to any penalty for failing to comply with a collection of information if it does not display a currently valid OMB control number.</p> <p>PLEASE DO NOT RETURN YOUR FORM TO THE ABOVE ADDRESS.</p>						
1. REPORT DATE (DD-MM-YYYY) 23-09-2004		2. REPORT TYPE Reprint		3. DATES COVERED (From - To)		
4. TITLE AND SUBTITLE The Linear Dependence of the Post-sunset Equatorial Anomaly Electron Density on Solar Flux and Its Relation to the Maximum Pre-reversal E x B Drift Velocity Through Its Dependence on Solar Flux				5a. CONTRACT NUMBER		
				5b. GRANT NUMBER		
				5c. PROGRAM ELEMENT NUMBER 61102F		
6. AUTHOR(S) James A. Whalen				5d. PROJECT NUMBER 1010 and 2311		
				5e. TASK NUMBER SD SD		
				5f. WORK UNIT NUMBER A1' A4		
7. PERFORMING ORGANIZATION NAME(S) AND ADDRESS(ES) Air Force Research Laboratory/VSBXP 29 Randolph Road Hanscom AFB, MA 01731-3010				8. PERFORMING ORGANIZATION REPORT NUMBER AFRL-VS-HA-TR-2004-1157		
9. SPONSORING/MONITORING AGENCY NAME(S) AND ADDRESS(ES)				10. SPONSOR/MONITOR'S ACRONYM(S)		
				11. SPONSOR/MONITOR'S REPORT NUMBER(S)		
12. DISTRIBUTION/AVAILABILITY STATEMENT Approved for Public Release; Distribution Unlimited.						
13. SUPPLEMENTARY NOTES REPRINTED FROM: JOURNAL OF GEOPHYSICAL RESEARCH, Vol 109, A07309, doi: 10.1029/2004JA010528.						
14. ABSTRACT The post sunset equatorial ionization anomaly, with maximum F layer electron density, Nemax, occurring near 2100 LT, has been found during solar maximum to be a linear function of the maximum pre-reversal E x B drift velocity (E x B drift). In order to examine this relation at all levels of solar flux, Nemax is measured during 13 years of an entire solar cycle by 8 ionospheric sounders located in anomaly in both north and south dip latitudes and in eastern Asia, the Pacific and South America. At each location the monthly median Nemax increases linearly with the monthly average solar flux, Sa, over the range from 70 to 285 sfu. The linear function varies markedly with location, and by month at each location. The relation of E x B drift, which is also a linear function of Sa, is determined using measurements of Nemax vs. Sa measured at Bogota in the anomaly plotted as a function of E x B vs. Sa measured at Jicamarca at the dip equator. The result is that Nemax is a linear function of E x B, which is in agreement with that found previously during solar maximum. Accordingly, the Nemax vs. E x B relation is independent of Sa. The fact that Nemax is linear in Sa at each site implies Nemax is linear in E x B at each, but with a functional dependence that varies with latitude and longitude.						
15. SUBJECT TERMS Equatorial ionosphere Solar cycle Ionospheric dynamics Scintillation Equatorial spread F						
16. SECURITY CLASSIFICATION OF:			17. LIMITATION OF ABSTRACT	18. NUMBER OF PAGES	19a. NAME OF RESPONSIBLE PERSON	
a. REPORT UNCL	b. ABSTRACT UNCL	c. THIS PAGE UNCL			James A. Whalen	
			UNL		19b. TELEPHONE NUMBER (Include area code) (781) 377-4766	

Linear dependence of the postsunset equatorial anomaly electron density on solar flux and its relation to the maximum prereversal $\mathbf{E} \times \mathbf{B}$ drift velocity through its dependence on solar flux

James A. Whalen

Space Vehicles Directorate, Air Force Research Laboratory, Hanscom Air Force Base, Massachusetts, USA

Received 5 April 2004; accepted 3 June 2004; published 30 July 2004.

[1] The postsunset equatorial ionization anomaly, with maximum F layer electron density, N_{max} , occurring near 2100 LT, has been found during solar maximum to be a linear function of the maximum prereversal $\mathbf{E} \times \mathbf{B}$ drift velocity ($\mathbf{E} \times \mathbf{B}$ drift). In order to examine this relation at all levels of solar flux, N_{max} is measured during 13 years of an entire solar cycle by eight ionospheric sounders located in the anomaly in both north and south dip latitudes and in eastern Asia, the Pacific, and South America. At each location the monthly median N_{max} increases linearly with the monthly average solar flux, S_a , over the range from 70 to 285 sfu. The linear function varies markedly with location and by month at each location. The relation to $\mathbf{E} \times \mathbf{B}$ drift, which is also a linear function of S_a , is determined using measurements of N_{max} versus S_a measured at Bogota in the anomaly plotted as a function of $\mathbf{E} \times \mathbf{B}$ versus S_a measured at Jicamarca at the dip equator. The result is that N_{max} is a linear function of $\mathbf{E} \times \mathbf{B}$, which is in agreement with that found previously during solar maximum. Accordingly, the N_{max} versus $\mathbf{E} \times \mathbf{B}$ relation is independent of S_a . The fact that N_{max} is linear in S_a at each site implies N_{max} is linear in $\mathbf{E} \times \mathbf{B}$ at each but with a functional dependence that varies with latitude and longitude. **INDEX TERMS:** 2415 Ionosphere: Equatorial ionosphere; 2411 Ionosphere: Electric fields (2712); 2437 Ionosphere: Ionospheric dynamics; 2439 Ionosphere: Ionospheric irregularities; 7536 Solar Physics, Astrophysics, and Astronomy: Solar activity cycle (2162); **KEYWORDS:** equatorial anomaly, solar cycle, solar flux, $\mathbf{E} \times \mathbf{B}$ drift

Citation: Whalen, J. A. (2004), Linear dependence of the postsunset equatorial anomaly electron density on solar flux and its relation to the maximum prereversal $\mathbf{E} \times \mathbf{B}$ drift velocity through its dependence on solar flux, *J. Geophys. Res.*, 109, A07309, doi:10.1029/2004JA010528.

1. Introduction

[2] The postsunset equatorial ionization anomaly consisting of the two bands of enhanced F layer electron density that parallel the dip equator was identified through ionospheric soundings by Appleton [1954]. Its description was greatly advanced by the ionospheric sounders in place during the International Geophysical Year (IGY) of 1957–1958 [Wright, 1962; Rao, 1963]. Its significance as the highest F layer electron density on the planet has inspired numerous observational and theoretical studies [Kelley, 1989; Doherty *et al.*, 1997], and its role as the locus of maximum scintillation on transionospheric RF propagation has further stimulated continued interest [Aarons, 1993].

[3] The highest level of scintillation occurs at the intersection of the anomaly with an equatorial bubble, both of which are products of the postsunset eastward electric field and the resulting upward $\mathbf{E} \times \mathbf{B}$ drift velocity. However, whereas the anomaly is basically determined by the drift velocity, bubbles require an additional stimulus probably by gravity waves

[Tsunoda, 1981; Whalen, 2000]. As a result, bubble occurrence and the resulting scintillation are essentially random.

[4] Although essential to understanding and hence predicting scintillation, the maximum prereversal $\mathbf{E} \times \mathbf{B}$ drift velocity ($\mathbf{E} \times \mathbf{B}$) is difficult to measure. This is because it occurs within a brief local time (LT) window generally between 1830 and 1930 LT. As this window moves westward with the terminator, only a few ground stations are situated near enough to the dip equator to measure $\mathbf{E} \times \mathbf{B}$ drift, so it is available at only a few isolated longitudes and universal times (UTs). Satellites can measure this maximum drift velocity but only sporadically, since the local time latitude windows are so narrow. In short, this parameter is essentially never available in any given time and longitude. Given its importance, the alternative is to seek observations that make possible its inference.

[5] The parameter most quantitatively related to $\mathbf{E} \times \mathbf{B}$ drift has been found to be the magnitude of the maximum F layer electron density of the crest of the anomaly at the time of its maximum latitudinal extent, which occurs near 2100 LT [Whalen, 2001]. This result, based on the study of a month, has been extended to an entire year at solar maximum using the daily measurements of N_{max} , N_{mF2}

at ~ 2100 LT, at a single location near the nominal anomaly crest, Bogota at 16.0° dip latitude (DLAT) [Whalen, 2003]. The daily measurements have been organized into the six categories of $\mathbf{E} \times \mathbf{B}$ drift, measured at Jicamarca by Fejer *et al* [1999] also during solar maximum: two in magnetic activity $K_p < 3$ and $K_p > 3$ and three in seasons designated as E (March, April, September, and October), D (November to February), and J (May to August).

[6] Nemax was found to increase linearly with $\mathbf{E} \times \mathbf{B}$ drift with season in the order from J to D to E at a given K_p and with magnetic activity from $K_p > 3$ to $K_p < 3$ at a given season. In the J months, Nemax was nearly independent of K_p . As a result, irrespective of whether the variation of $\mathbf{E} \times \mathbf{B}$ is caused by magnetic activity or by season, the anomaly responds linearly to its magnitude alone. Thus statistically, the measurement of Nemax implies $\mathbf{E} \times \mathbf{B}$ drift and vice versa.

[7] A further result was that the probability of every level of equatorial spread F , in particular of macroscopic bubbles, increased approximately linearly with Nemax and therefore with $\mathbf{E} \times \mathbf{B}$, with the possible exception of the D months [Whalen, 2003]. That is, Nemax also yielded the probability of occurrence of the phenomena that produce maximum scintillation.

[8] Because of the importance of Nemax seen during solar maximum, this paper will determine its properties throughout an entire solar cycle: first, its dependence on solar flux and second, its relation to $\mathbf{E} \times \mathbf{B}$ at all levels of solar flux. In outline, section 2 describes the ionospheric sounders used in the experiment, section 3 describes the variation of solar flux by month over the 13 year period studied, section 4 describes the variation of Nemax over this period, section 5 describes the dependence of Nemax on solar flux as being linear at all sites, section 6 describes the relation of Nemax to $\mathbf{E} \times \mathbf{B}$ and that its linearity with S_a is a result of the linearity of $\mathbf{E} \times \mathbf{B}$ with solar flux, and section 7 gives summary and conclusions.

2. Experiment

[9] Eight ionospheric sounders are employed in this study, as shown in both geographic and geomagnetic coordinates in Figure 1. Each measures the F layer critical frequency, foF2, which is the maximum plasma frequency from which the maximum F layer electron density is derived. Also shown is the Jicamarca Incoherent Scatter Radar that measures $\mathbf{E} \times \mathbf{B}$ drift. The sounders are all those located in the anomaly with useable data that was available in the archives for the entire period studied.

3. Solar Flux

[10] The period of the observations is an entire solar cycle starting during the International Geophysical Year (IGY) at 1957 near the maximum of solar cycle 19, the highest solar maximum observed to date. It extends through the solar minimum during the International Year of the Quiet Sun (IQSY) in 1963 and ends near the maximum of cycle 20 in 1970 (Figure 2). The points are the monthly mean observed solar flux, and the solid curve is the yearly running average. The arrows identify the period of the study during which S_a

varies between 70 and 285 10.7-cm solar flux units (sfu) of $10^{-22} \text{ W m}^{-2} \text{ Hz}^{-1}$.

4. Measurement of Nemax

[11] Nemax, NmF2 at its maximum near 2100 LT, is derived from the monthly median foF2, recorded in individual graphs and tabulations in the ionospheric data published by the National Oceanic and Atmospheric Administration. The database for the eight sounders described here consists of approximately 1200 measurements. The availability of the data is a result of the remarkable cooperative international scientific effort of IGY that persisted in part through IQSY and beyond.

[12] The solar maximum study by Whalen [2003] used measurements of Nemax at Bogota and of $\mathbf{E} \times \mathbf{B}$ at Jicamarca, and the same two locations yield the two parameters here. However, because the Bogota measurements are not available as continuously throughout this period as are those at Taipei, data from the latter will be examined in the most complete detail. The results from the two locations will be seen below to be very similar.

[13] The monthly median Nemax measured at Taipei yearly from 1957 through 1969 is shown in Figure 3. Both seasonal and solar cycle effects are evident: Nemax is maximum near the equinoxes, minimum near June, and intermediate near December, and maximum at the solar maximum of 1957–1958, decreasing to its minimum at the solar minimum near 1963, increasing to a lesser maximum near the ill-defined and lesser solar maximum near 1969. At solar minimum the seasonal variation all but disappears and is not evident again until about 1965 to 1966, with a marked increase in 1967.

[14] Because Nemax is continuously changing with both season and solar flux, its dependence on either separately is not evident. Accordingly, the approach here will be to determine the relation of Nemax to S_a for each month over the entire 13 year period.

5. Linear Dependence of Nemax on Solar Flux by Month

5.1. Taipei

[15] Nemax measured at Taipei beginning with January 1957 is plotted versus S_a also measured on January 1957, and this process is repeated for the January of each of the following 12 years. The result is shown in Figure 4 in which each point, labeled by year, is connected in yearly succession by the dashed line. The agreement with the straight line, which is the least squares fit, indicates that Nemax varies as a linear function of S_a for January over the entire solar cycle.

[16] The procedure of Figure 4 is repeated for each of the other months, and all 12 are shown in Figure 5. Each is reasonably fit by a straight line, the largest departures being in March and April. The slopes vary markedly from month to month, those for June, July, and August being considerably smaller than the others, reflecting the fact that the small magnitude of Nemax for these months persists throughout the solar cycle.

5.2. Other Sounders

[17] The measurements of the four additional sounders in the Northern Hemisphere, Bogota, Paramaribo, Okinawa,

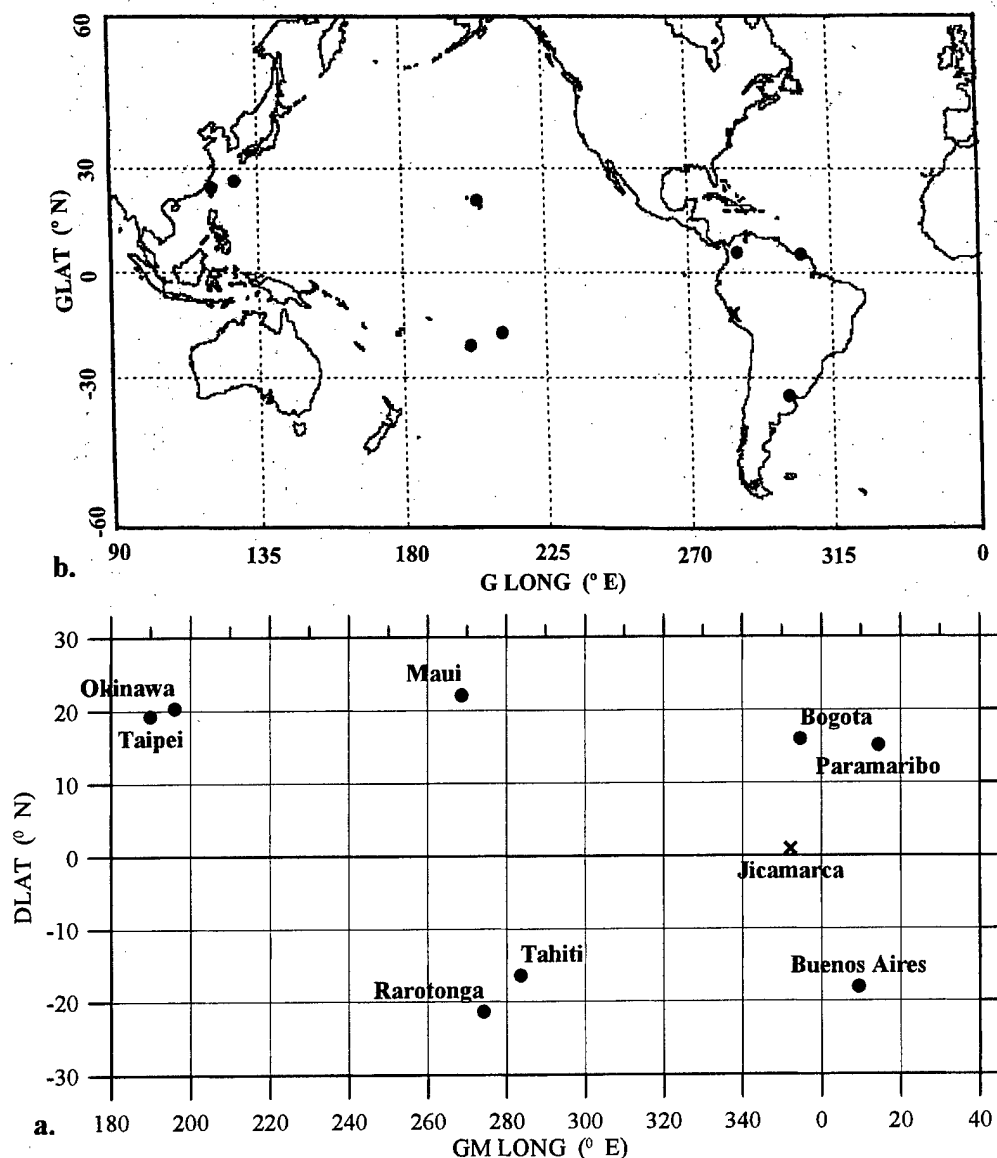


Figure 1. The eight ionospheric sounders employed in this study, together with the incoherent scatter radar at Jicamarca in (a) dip latitude (DLAT) versus geomagnetic longitude (GMLONG) and (b) geographic coordinates.

and Maui, are plotted in the format of Figure 5 in Figure 6. Nemax is linear in Sa at each location and for each month, although each differs markedly by location and month. The same is true for the three sounders in the Southern Hemisphere, Tahiti, Rarotonga, and Buenos Aires. The fact that the property of linearity is common to all implies a common source which is taken to be $\mathbf{E} \times \mathbf{B}$.

6. Relation of Nemax to $\mathbf{E} \times \mathbf{B}$ Drift

6.1. $\mathbf{E} \times \mathbf{B}$ Drift Linearity by Season

[18] $\mathbf{E} \times \mathbf{B}$ is itself a linear function of solar flux as measured at the dip equator at Kodiakanal by *Ramesh and Sastri* [1995] and at Jicamarca by *Fejer et al.* [1996]. Since Nemax and $\mathbf{E} \times \mathbf{B}$ are both linear functions of Sa, the

implication is that the relation between the two will be linear. This will be examined here to see to what extent it has a quantitative basis and how well it agrees with previous measurements that are independent of Sa. Considered here will be Nemax at Bogota in the anomaly and $\mathbf{E} \times \mathbf{B}$ drift at Jicamarca near the equator, both of which are at the same longitude.

6.2. Nemax and $\mathbf{E} \times \mathbf{B}$ as Functions of Solar Flux

[19] In order to conform to the format of the Jicamarca data, the measurements of Nemax at Bogota in Figure 6 are combined into the three seasons E, D, and J, as shown in Figure 7a. The points are more scattered than those in the individual months because the linear relations differ by month within each season.

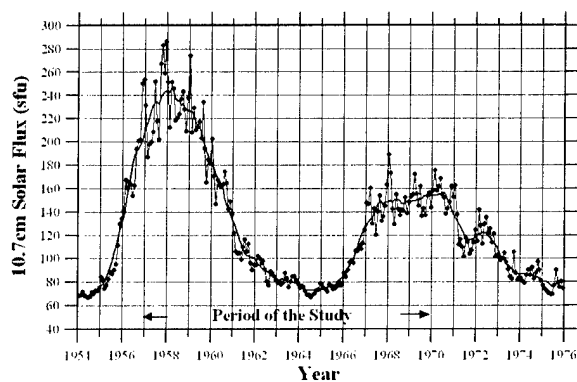


Figure 2. Solar flux during cycles 19 and 20 showing the period studied, 1957 through 1969. Points are the monthly mean observed solar fluxes, and the solid curve is the yearly running average.

[20] Values of $E \times B$ measured at Jicamarca for the same three seasons are shown in Figure 7b (after *Fejer et al.* [1996]). Each point is the average of the observations (the number of which is shown by each point), and the bars are the standard deviations.

[21] Nemax versus Sa is very similar to $E \times B$ versus Sa in the sense that both increase linearly with Sa, and the dependence on Sa, as indicated by the slope, decreases in the order E to D to J. An important difference is that Nemax is measured at all levels of magnetic activity, but $E \times B$ is only measured for $K_p < 3$. The effects of this difference will be seen below.

6.3. Nemax Versus $E \times B$ Via the Dependence of Each on Solar Flux

[22] To examine the relation more quantitatively, Nemax at a given Sa (from Figure 7a) is plotted versus $E \times B$ at that same Sa (from Figure 7b) for a succession of values of Sa, a process that is repeated for each of the E, D, and J months. The resulting three linear relations of Nemax versus $E \times B$ are shown together as the dashed lines in Figure 8. The three are in essential agreement given that the standard deviation in $E \times B$ for each is ~ 10 m/s. However, it is significant that the three have nearly the same slope and therefore are in agreement as to the dependence of Nemax on $E \times B$. Also, the fact that the E and D lines are displaced to higher $E \times B$ than the J is consistent with the difference in magnetic activity of the measurements, $E \times B$ only at $K_p < 3$ but Nemax at all levels of K_p .

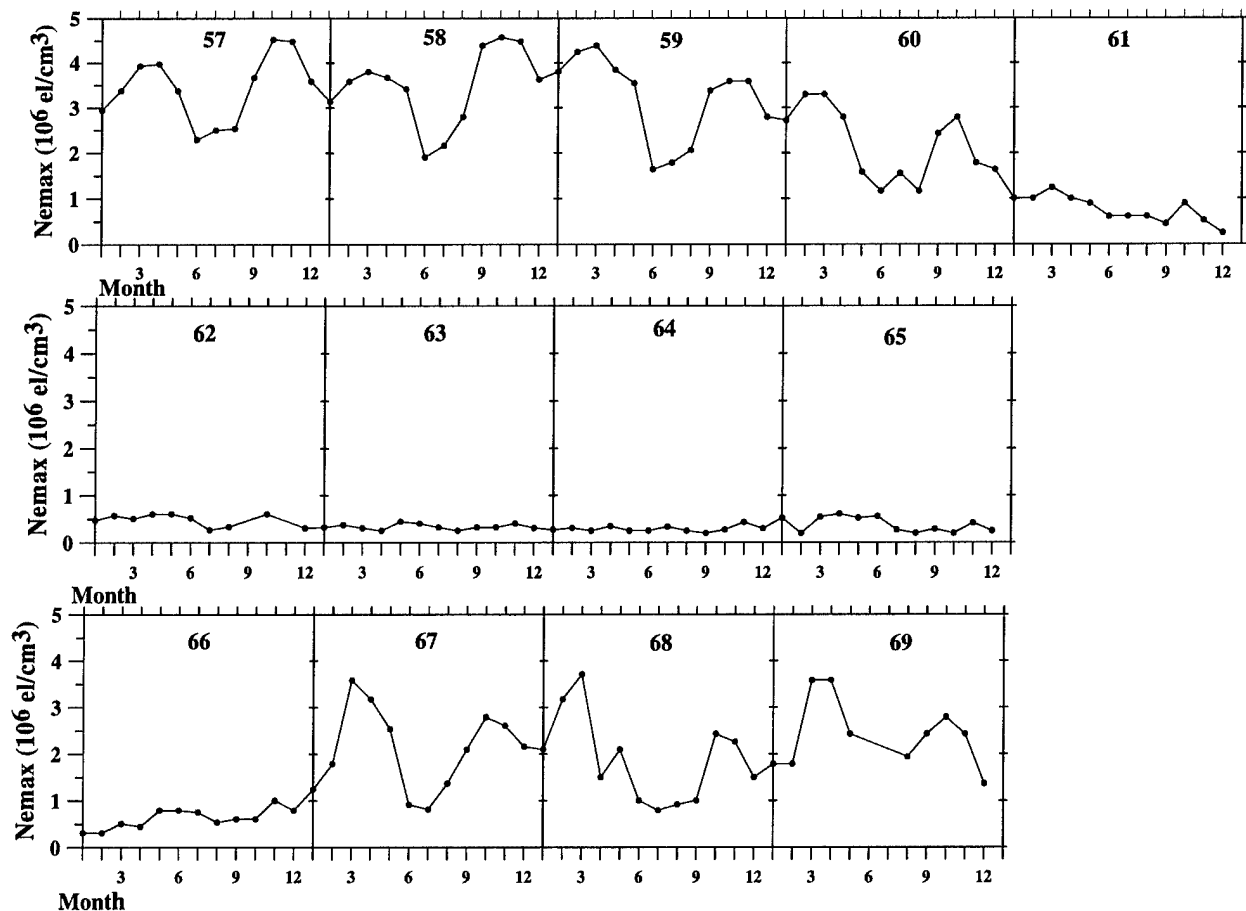


Figure 3. Monthly median Nemax at Taipei 1957 through 1969. Two major influences are evident: season in which Nemax is maximum in the equinoxes, minimum near June, and intermediate near December, and solar cycle, in which Nemax is maximum at solar maximum, minimum at solar minimum, and in general follows the trend of solar flux.

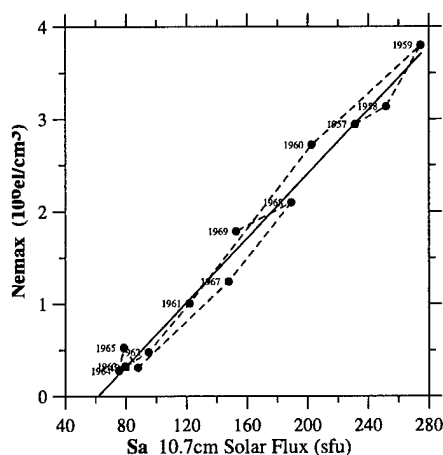


Figure 4. The linearity of Nemax with solar flux for January. Nemax measured at Taipei on January of each year plotted versus Sa measured on the corresponding January for each of the 13 years spanning the solar cycle. The dashed line connects in succession the points that are labeled by year. The straight line is the least squares fit.

[23] As described in section 1, as K_p increases from <3 to >3 , $E \times B$ undergoes a decrease that is greatest for E months, less for D months, and nearly nil for J months. Therefore the inclusion of measurement at $K_p > 3$ at a given Sa in the $E \times B$ versus Sa relations of Figure 7b would reduce the value of $E \times B$ at that level of Sa. As a result, Nemax at that level of Sa would be plotted at a lower value of $E \times B$. The effect would be to translate both E and D lines to lower values of $E \times B$ but not the J because of its near-independence on K_p . Such a correction would bring the three into better agreement with one another and therefore more nearly independent of season. Seasonal independence was also found in the earlier solar maximum study [Whalen, 2003], and the following comparison will further test the consistency of the present results.

6.4. Comparison With Solar Maximum Results

[24] Nemax measured daily at Bogota during the solar maximum year of 1958 was found to be a linear function of $E \times B$ measured at Jicamarca, also during solar maximum. The result (from Figure 4 of Whalen [2003]) is shown as the solid straight line in Figure 8; the points are median values, and the bars are the upper and lower quartiles. The quartiles have the nearly the same dependence on $E \times B$ drift as the medians, a property also of the deciles.

[25] This slope is nearly the same as that of the individual seasons, which indicates agreement as to the dependence of Nemax on $E \times B$. Furthermore, the inclusion of the $E \times B$ measurements for $K_p > 3$ described above, which would bring the magnitude of the E, D, and J months into better agreement with one another, would also bring them into better agreement with this 1958 data, which are inclusive of season and of K_p . Altogether, this is considerable agreement, given the independent sources of data.

[26] Accordingly, the relation of Nemax to $E \times B$ inferred from the separate dependence of each on Sa is in essential agreement with the relation determined from

the daily measurements during solar maximum. Thus statistically, and subject to the large uncertainties, it is possible to conclude that Nemax is linear in Sa because it is linear in $E \times B$, which is itself linear in Sa, and furthermore that the Nemax versus $E \times B$ relation found during solar maximum is independent of Sa.

7. Discussion

[27] The above agreement is evidence that Nemax at Bogota is the same linear function of $E \times B$ at Jicamarca throughout the entire range of Sa. The result is that $E \times B$ at Jicamarca can be inferred from Nemax at Bogota under nearly all conditions of solar flux not only seasonally but also monthly.

[28] These results indicate further that the linearity of Nemax with $E \times B$ is not limited to the longitude sector of Bogota and Jicamarca because both parameters are observed elsewhere to be linear with Sa: Nemax at the longitudes of all eight sounders and $E \times B$ at the longitudes of Jicamarca and Kodiakanal by Ramesh and Sastri [1995] and by Sastri [1996]. Accordingly, the results imply that Nemax is linear in $E \times B$ in general. However, the functional relation can be expected to depend on longitude as well as latitude.

[29] The dependence of $E \times B$ versus Sa on longitude is evident in the comparison between Jicamarca and Kodiakanal as noted above and even more extensively with longitude as indicated by Scherliess and Fejer [1999]. The dependence of Nemax versus $E \times B$ on latitude was seen in the comparison between Bogota at 16.0° DLAT and Panama at 20.3° DLAT which are at the same longitude [Whalen, 2003]. Here the dependence of Nemax on $E \times B$ is much smaller at Panama than at Bogota as a result of its location at the high-latitude edge of the anomaly.

[30] These results support the prospect that the measurement of Nemax can be used to infer $E \times B$ drift over a large range of solar flux. This includes ionospherically or photometrically and in particular the ultraviolet images of the postsunset anomaly by the Special Sensor Ultraviolet Spectrographic Imager (SSUSI) [Christensen et al., 2003].

[31] It is not possible here to measure the occurrence of bubbles which could imply the dependence of scintillation on Sa. However, DasGupta et al. [1981] find scintillation near the anomaly crest in the Indian sector to increase approximately linearly with Sa over the range ~ 75 –200 sfu and to have a seasonal dependence similar to that found here both in Nemax and in $E \times B$. Accordingly, Nemax and $E \times B$ appear to be in a linear relation to bubble occurrence over the solar cycle similar to that found at solar maximum by Whalen [2003].

8. Summary

[32] The electron density of the postsunset equatorial anomaly at its maximum near 2100 LT, Nemax, is a linear function of solar flux, as observed at each of eight ionospheric sounders for each month during 13 years as Sa varies from 75 to 250 sfu. The linear dependence varies by location and by month at each location.

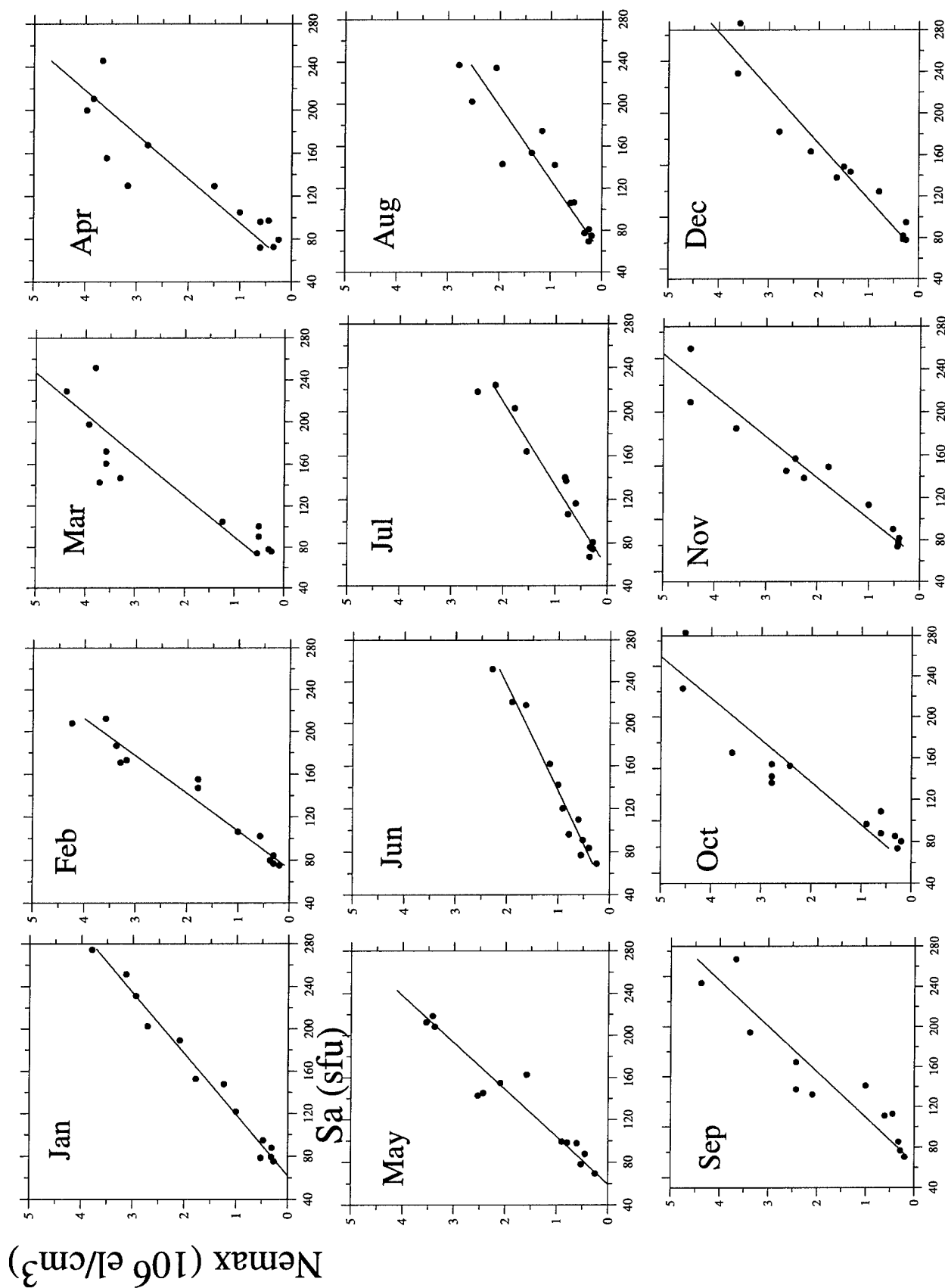


Figure 5. The plot shown in Figure 4 for all months. The linearity of N_{max} versus S_a is common to all months, but the slope is different for each.

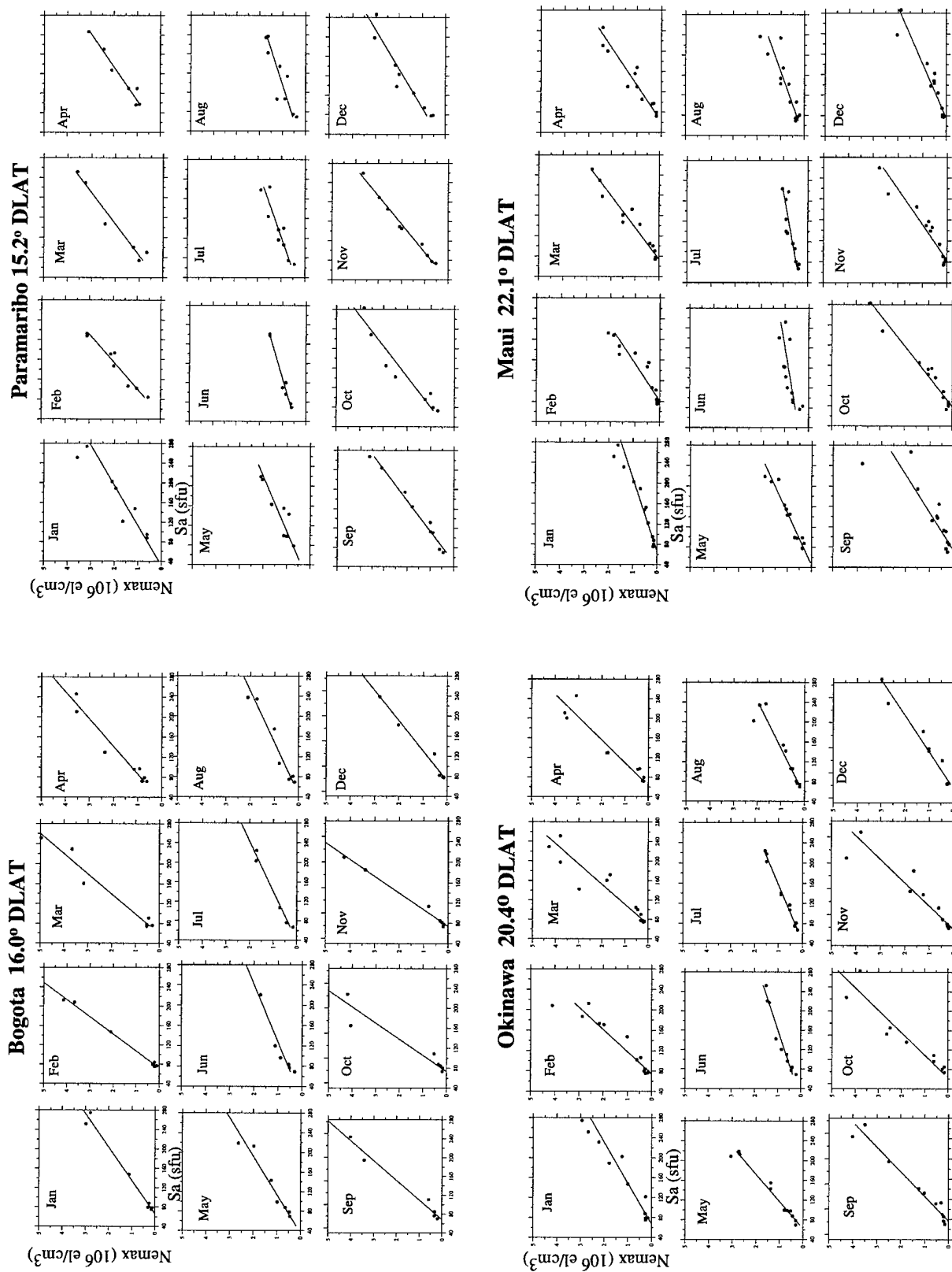


Figure 6. The four additional Northern Hemisphere sounders shown in the format of Figure 5. The linearity is common to all sites, but differs by location and by month.

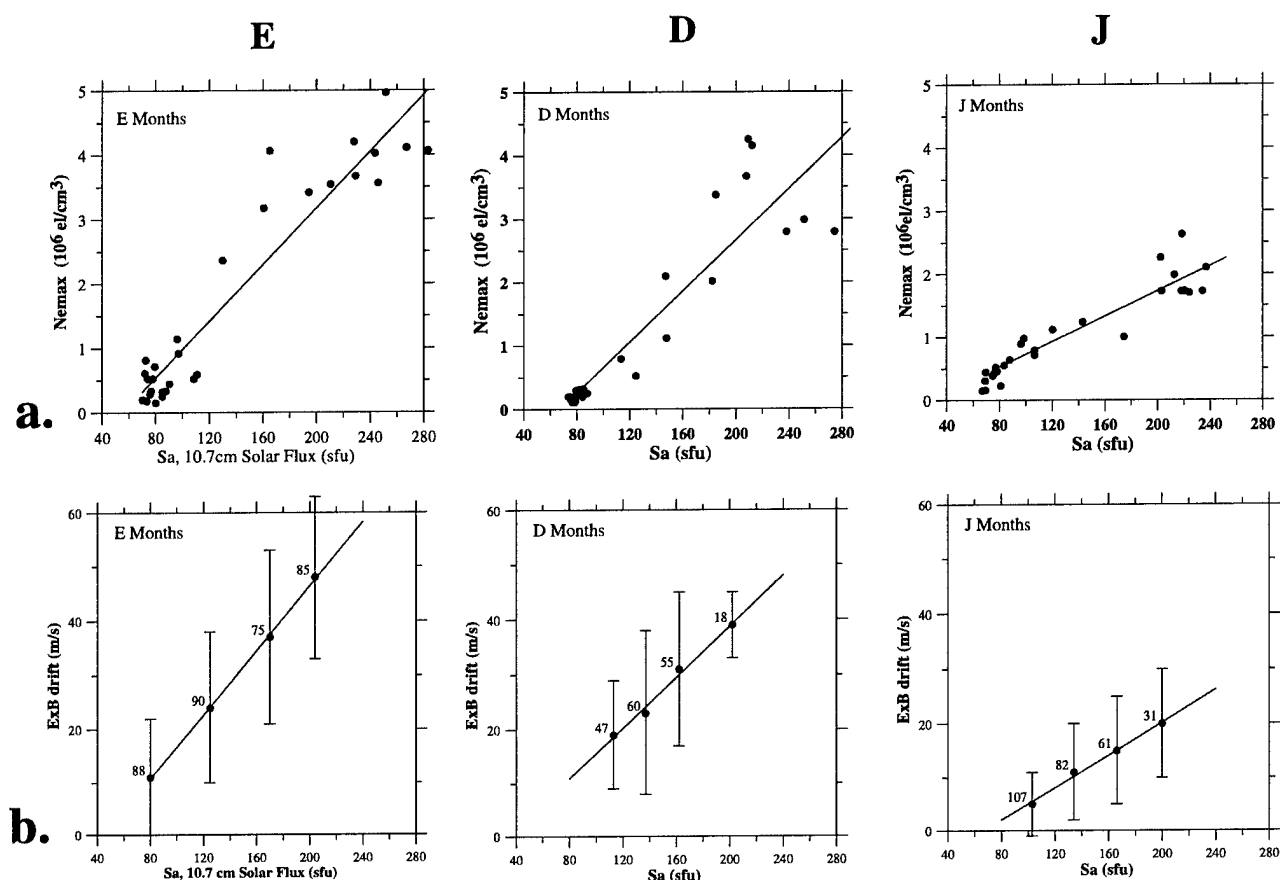


Figure 7. Comparison by season of the linear dependence on solar flux of both Nemax and of $\mathbf{E} \times \mathbf{B}$. (a) The observations of Nemax at Bogota of Figure 6 combined by season, as E, D, and J. (b) Jicamarca maximum prereversal $\mathbf{E} \times \mathbf{B}$ drift velocity in the same seasons [after Fejer *et al.*, 1996].

[33] The linearity in Nemax with Sa is the result of the linearity of $\mathbf{E} \times \mathbf{B}$ with Sa, as determined via the separate dependence of each on Sa, Nemax at Bogota, and $\mathbf{E} \times \mathbf{B}$ at Jicamarca. The resulting Nemax versus $\mathbf{E} \times \mathbf{B}$ is in addition consistent with that found at solar maximum. Accordingly, statistically and within the uncertainties, Nemax versus $\mathbf{E} \times \mathbf{B}$ is independent of Sa. The fact that Nemax is linear with Sa at each anomaly site implies that Nemax is linear in $\mathbf{E} \times \mathbf{B}$ at each but with functional dependence that differs with latitude and longitude.

Appendix A: Influence of Daytime NmF2 on Nemax

[34] Nemax consists of plasma ionized by solar radiation, so it is necessary to understand how the dependence of daytime plasma on Sa affects the measurement of Nemax. The problem occurs because daytime NmF2 also varies linearly with sunspot number [e.g., Ratcliffe and Weekes, 1960] as does the daytime total electron content [Bhonsle *et al.*, 1965]. Furthermore, the linear dependence is greatest in equinox, less in northern winter, and least in northern summer, a dependence which is very much like that seen here in Nemax and also in $\mathbf{E} \times \mathbf{B}$.

[35] In order to examine the importance of the daytime plasma, the latitudinal dependence of Nemax will be examined. It makes use of the fact that the linear relation of

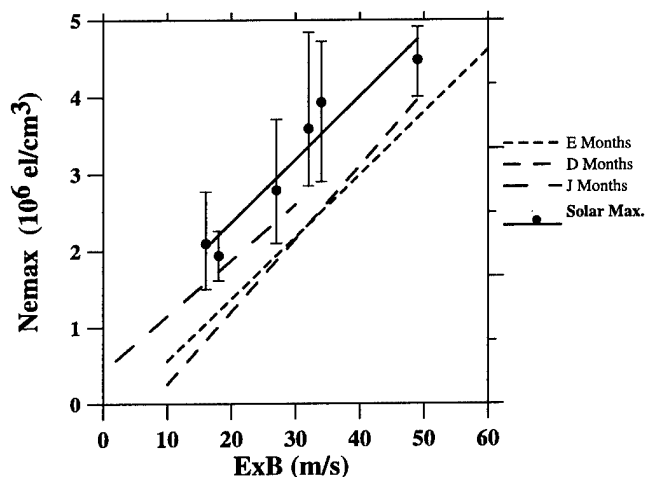


Figure 8. Nemax at Bogota versus $\mathbf{E} \times \mathbf{B}$ at Jicamarca derived from their mutual dependence on Sa compared with that measured during solar maximum. The three dashed straight lines, E, D, and J, are values are Nemax from Figure 7a plotted as a function of $\mathbf{E} \times \mathbf{B}$ from Figure 7b where each is expressed as a linear function of Sa. The points fit by the solid line result from daily measurements at solar maximum [Whalen, 2003]. The agreement is evidence that the relation of Nemax to $\mathbf{E} \times \mathbf{B}$ seen at solar maximum persists at all levels of solar flux.

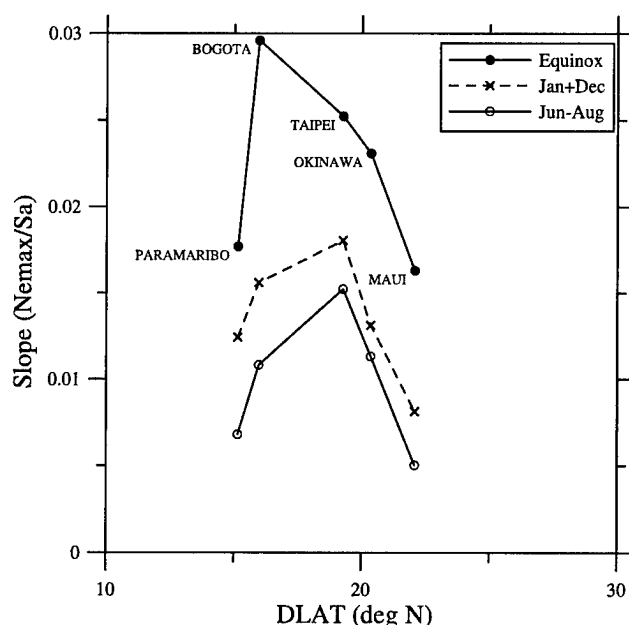


Figure A1. The slopes for each of the Northern Hemisphere sounders for each of three seasons plotted versus DLAT. The organization into quasi-latitude profiles in magnetic coordinates is evidence that the principal cause of the linearity of Nemax on Sa is $\mathbf{E} \times \mathbf{B}$ and not the daytime plasma.

Nemax versus Sa can be described by two parameters, the slope of the line and a point. Taking the point as the minimum Nemax at 75 sfu, which is nearly constant by month, the essential variation of Nemax over the range of Sa can be described by the slope alone. The procedure is to plot the slope at each Northern Hemisphere location versus DLAT.

[36] The slopes of the five Northern Hemisphere sounders for each of three seasonal periods, equinox, January to December, and June to August, is plotted versus DLAT in Figure A1. Each sounder is identified on the equinox distribution. The slope for each season increases with DLAT from Paramaribo to Bogota and decreases from Taipei to Okinawa to Maui. Even though the DLAT coordinates can be considered to be only approximate for the large longitudinal extent, the slopes form quasi-latitudinal profiles not unlike those observed in Nemax on individual days by a latitudinal chain of ionospheric sounders [e.g., Whalen, 2001].

[37] The daytime plasma could not explain the observed dependence on DLAT, so its overall effect is evidently small. Accordingly, the slopes have a clear dependence on magnetic latitude, so Nemax is consistent with the anomaly and therefore with $\mathbf{E} \times \mathbf{B}$.

[38] **Acknowledgments.** The data used here resulted from the unparalleled international cooperative scientific program of the IGY that persisted through IQSY and beyond. This work was sponsored in part by the Air Force Office of Scientific Research task 211AS.

[39] Arthur Richmond thanks Patricia Doherty and another reviewer for their assistance in evaluating this paper.

References

- Aarons, J. (1993), The longitudinal morphology of equatorial F layer irregularities relevant to their occurrence, *Space Sci. Rev.*, **64**, 314.
- Appleton, E. V. (1954), The anomalous equatorial belt in the F2 layer, *J. Atmos. Terr. Phys.*, **5**, 348.
- Bhonsle, R. V., A. V. da Rosa, and O. K. Garriott (1965), Measurements of the total electron content and the equivalent slab thickness of the midlatitude ionosphere, *NBS J. Res. Radio Sci.*, **69D**, 927.
- Christensen, X., et al. (2003), Initial observations with the Global Ultraviolet Imager (GUVI) in the NASA TIMED satellite mission, *J. Geophys. Res.*, **108**(A12), 1451, doi:10.1029/2003JA009918.
- DasGupta, A., A. Maitra, and S. Basu (1981), Occurrence of nighttime VHF scintillations near the equatorial anomaly crest in the Indian sector, *Radio Sci.*, **6**, 1455–1458.
- Doherty, P. H., D. N. Anderson, and J. A. Klobuchar (1997), Total electron content over the Pan-American longitudes: March–April 1994, *Radio Sci.*, **32**, 1597–1606.
- Fejer, B. G., E. R. de Paula, L. Scherliess, and I. S. Batista (1996), Incoherent scatter radar, ionosonde, and satellite measurements of equatorial E region vertical plasma drifts in the evening sector, *Geophys. Res. Lett.*, **14**, 1733–1736.
- Fejer, B. G., L. Scherliess, and E. R. de Paula (1999), Effects of the vertical plasma drift velocity on the generation and evolution of equatorial spread F, *J. Geophys. Res.*, **104**, 19,859–19,869.
- Kelley, M. C. (1989), *The Earth's Ionosphere, Plasma Physics and Electrodynamics*, Academic, San Diego, Calif.
- Ramesh, K. B., and J. H. Sastri (1995), Solar cycle variations in F-region vertical drifts over Kodaikanal, India, *Ann. Geophys.*, **13**, 633–640.
- Rao, B. C. N. (1963), Some characteristic features of the equatorial ionosphere and the location of the F region equator, *J. Geophys. Res.*, **68**, 2541–2549.
- Ratcliffe, J. A., and K. Weekes (1960), The ionosphere, in *Physics of the Ionosphere*, edited by J. A. Ratcliffe, p. 378–470, Academic, San Diego, Calif.
- Sastri, H. S. (1996), Longitudinal dependence of equatorial F region vertical plasma drifts in the dusk sector, *J. Geophys. Res.*, **101**, 2445–2452.
- Scherliess, L., and B. G. Fejer (1999), Radar and satellite global equatorial F region vertical drift model, *J. Geophys. Res.*, **104**, 6829–6842.
- Tsunoda, R. T. (1981), Time evolution and dynamics of equatorial backscatter plumes: 1. Growth phase, *J. Geophys. Res.*, **86**, 139.
- Whalen, J. A. (2000), An equatorial bubble: Its evolution observed in relation to bottomside spread F and to the Appleton anomaly, *J. Geophys. Res.*, **105**, 5303–5315.
- Whalen, J. A. (2001), The equatorial anomaly: its quantitative relation to equatorial bubbles, bottomside spread F and $\mathbf{E} \times \mathbf{B}$ drift velocity during a month at solar maximum, *J. Geophys. Res.*, **106**, 29,125–29,132.
- Whalen, J. A. (2003), The dependence of the equatorial anomaly and of equatorial spread F on the maximum prereversal $\mathbf{E} \times \mathbf{B}$ drift velocity measured at solar maximum, *J. Geophys. Res.*, **108**(A5), 1193, doi:10.1029/2002JA009755.
- Wright, J. W. (1962), Vertical cross-sections of the ionosphere across the geomagnetic equator, *Natl. Bur. of Stand. Tech. Note 138*, U.S. Dept. of Commerce, Washington, D.C.

J. A. Whalen, Space Vehicles Directorate, Air Force Research Laboratory, 29 Randolph Road, Hanscom Air Force Base, MA 01731-3010, USA. (james.whelen@hanscom.af.mil)